0026-895X/01/5905-1100–1107$3.00
MOLECULAR PHARMACOLOGY
Copyright © 2001 The American Society for Pharmacology and Experimental Therapeutics
Mol Pharmacol 59:1100–1107, 2001

Vol. 59, No. 5
526/899062
Printed in U.S.A.

MOL PHARM

Disparate Role of Na^+ Channel D2-S6 Residues in Batrachotoxin and Local Anesthetic Action

SHO-YA WANG, MARIA BARILE, and GING KUO WANG

Department of Biology, State University of New York at Albany, Albany, New York (S.-Y.W.); and Department of Anesthesia, Harvard Medical School and Brigham & Women's Hospital, Boston, Massachusetts (M.B., G.K.W.)

Received August 28, 2000; accepted January 23, 2001

This paper is available online at http://molpharm.aspetjournals.org

ABSTRACT

Batrachotoxin (BTX) stabilizes the voltage-gated Na^+ channels in their open conformation, whereas local anesthetics (LAs) block Na^+ conductance. Site-directed mutagenesis has identified clusters of common residues at D1-S6, D3-S6, and D4-S6 segments within the α-subunit Na^+ channel that are critical for binding of these two types of ligands. In this report, we address whether segment D2-S6 is similarly involved in both BTX and LA actions. Thirteen amino acid positions from G783 to L795 of the rat skeletal muscle Na^+ channel (μ1/Skm1) were individually substituted with a lysine residue. Four mutants (N784K, L785K, V787K, and L788K) expressed sufficient Na^+ currents for further studies. Activation and/or inactivation gating was altered in mutant channels; in particular, μ1-V787K displays enhanced slow inactivation and exhibited use-dependent inhibition of peak Na^+ currents during repetitive pulses. Two of these four mutants, μ1-N784K and μ1-L788K, were completely resistant to 5 μM BTX. This BTX-resistant phenotype could be caused by structural perturbations induced by a lysine point mutation in the D2-S6 segment. However, these two BTX-resistant mutants remained quite sensitive to bupivacaine block with affinity for inactivated Na^+ channels (K_I) of ~10 μM or less, which suggests that μ1-N784 and μ1-L788 residues are not in close proximity to the LA binding site.

MOLECULAR PHARMACOLOGY

Downloaded from molpharm.aspetjournals.org by guest on December 1, 2012

The voltage-gated Na^+ channels are membrane proteins responsible for the generation of action potentials in excitable membranes. In mammalian cells, the Na^+ channel family contains one large α subunit and one or two smaller β auxiliary subunits (β1, β2) (Catterall, 2000). The α-subunit clone consists of about 2000 amino acids and, when expressed alone in mammalian cells, exhibits functional Na^+ currents with gating kinetics comparable with those of the native Na^+ channels. The α-subunit primary sequence contains four homologous domains (D1–D4), each with six transmembrane segments (S1–S6) (Fig. 1A). Current structural models suggest that the Na^+ channel is organized as a pseudotetramer with S6 segments possibly lining the internal vestibule of the pore.

Local anesthetics (LAs) block voltage-gated Na^+ channels in a complicated state-dependent manner. LAs seem to have higher affinities toward open and inactivated states (Strichartz, 1973; Courtney, 1975). In contrast, a steroidal alkaloid toxin, batrachotoxin (BTX), isolated from poison-dart frogs, inhibits both Na^+ channel fast and slow inactivation and shifts the activation threshold to the hyperpolarizing direction (Khodorov, 1978). Consequently, the Na^+ channel opens readily with BTX present, even at the resting membrane potential. The receptors for LAs and BTX have been mapped within S6 segments of domains D1, D3, and D4 with several common residues important for binding of both LAs and BTX (Fig. 1B; Ragsdale et al., 1994; Wang and Wang, 1998, 1999; Linford et al., 1998; Vedantham and Cannon, 2000; Wang et al., 2000). Furthermore, a quaternary derivative of lidocaine, QX-314, can access the LA receptor of the neuronal Na^+ channels only via internal application (Strichartz, 1973). These findings together imply that S6 segments are closely aligned to form the internal vestibule of the Na^+ permeation pathway. Detailed mapping of S6 segments may therefore reveal the architecture of this pore region.

The fact that LAs can accelerate the dissociation rate of BTX from its receptor (Postma and Catterall, 1984) suggests that both LAs and BTX can bind simultaneously. Consistent with this result, LAs block single, BTX-modified Na^+ channels incorporated in lipid bilayers, apparently in a one LA to one BTX-modified channel relationship (Moczydlowski et al., 1986; Wang, 1988). The previous explanation for these observations is that BTX allosterically affects the binding affinity of LAs toward their receptor in Na^+ channels and vice versa. However, recent studies based on site-directed mutagenesis now revise this view. It was suggested that different surfaces of common residues are important for BTX and LA binding (Linford et al., 1998) or, alternatively, that common residues are involved in BTX and LA binding in a state-dependent

This study was supported by National Institutes of Health Grants GM35401 and GM48090.

ABBREVIATIONS: LA, local anesthetic; BTX, batrachotoxin; HEK, human embryonic kidney.

MOL PHARM
MOLECULAR PHARMACOLOGY
aspet

manner (Wang et al., 2000). Thus, studies of the involvement of S6 segments in BTX and LA actions will be essential for understanding the physiological consequences of these ligands.

In this report, we address two unsettled questions. First, we asked whether segment D2-S6 is involved in BTX action. We created a series of lysine mutants within this region and measured the mutants' BTX sensitivity. Two mutants became completely resistant to BTX modification. Second, we asked whether these BTX-resistant mutant channels also become resistant to LA. Surprisingly, they remained relatively sensitive to bupivacaine block.

Materials and Methods

Site-Directed Mutagenesis. Point mutations of a μ1 Na^+ channel clone (Trimmer et al., 1989) in a pcDNA1/Amp expression vector were performed as described previously (Nau et al., 1999) by means of the Transformer Site-Directed Mutagenesis Kit (CLONTECH, Palo Alto, CA). A mutagenesis primer and a restriction primer were used to generate the desired mutant. The potential mutants were selected and confirmed by DNA sequencing at the mutated site with appropriate primers.

Transient Transfection. The culture of HEK293t cells and their transient transfection were performed as described previously (Cannon and Strittmatter, 1993). Cells were first grown to 50% confluence in Dulbecco's modified Eagle's medium (Life Technologies, Grand Island, NY) containing 10% fetal bovine serum (HyClone, Logan, UT), 1% penicillin and streptomycin solution (Sigma, St. Louis, MO), 3 mM taurine, and 25 mM HEPES (Life Technologies). Transfection of these cells with μ1 (10 μg) and reporter plasmid CD8-pih3 m (1 μg) was accomplished by a calcium phosphate precipitation method in a Ti25 flask. Cells were replated 15 h after transfection, maintained at 37°C in a 5% CO_2 incubator, and used for experiments after 1 to 4 days, generally. However, mutant μ1-V787K usually did not express sufficient currents until day 4. Transfection-positive cells were identified by immunobeads (CD8-Dynabeads; Dynal, Lake Success, NY).

Whole-Cell Voltage Clamp. The whole-cell configuration of a patch-clamp technique (Hamill et al., 1981) was used to record Na^+ currents in cells coated with CD8 immunobeads. Experiments were performed at room temperature (23 ± 2°C). Glass electrodes contained 100 mM NaF, 30 mM NaCl, 10 mM EGTA, and 10 mM HEPES adjusted to pH 7.2 with CsOH. The electrodes had a tip resistance of 0.5 to 1.0 MΩ; access resistance was generally ≤ 2 to 3 MΩ. With series resistance compensation of 60 to 90%, the voltage error at +50 mV was < 4 mV on average. Series resistance errors with this magnitude are generally tolerable because quantitative measurements of current kinetics and drug block are insignificantly affected by such errors (Bean, 1992). The bath solution contained 65 mM NaCl, 85 mM choline chloride, 2 mM $CaCl_2$, and 10 mM HEPES adjusted to pH 7.4 with tetramethyl hydroxide. These ionic conditions resulted in smaller Na^+ currents at voltages from −60 to +10 mV, which in turn minimized the series resistance artifact in the conductance-voltage measurement. Stock solution of bupivacaine was prepared at 100 mM in aqueous solution and stored at −20°C until needed. BTX was prepared at 0.5 mM in dimethyl sulfoxide and stored at 4°C. Bupivacaine was purchased from Sigma, and BTX was a generous gift of Dr. John Daly (National Institutes of Health, Bethesda, MD). To conserve the use of BTX, we included this toxin in the pipette solution at 5 μM final concentration when needed. This toxin concentration was previously used to demonstrate the BTX-resistant phenotype in poison-dart frogs (Daly et al., 1980) and was high enough to modify >90% of available wild-type Na^+ channels under appropriate conditions. Whole-cell currents were recorded with Axopatch 200B, filtered at 5 kHz, and collected by pClamp software (Axon Instruments, Foster City, CA). In some experiments, currents were recorded by EPC-7. After gigaohm seal formation and establishment of whole-cell voltage clamp, the cells were dialyzed for ~20 min before data were acquired. Most of the capacitance and leakage current were canceled by the patch-clamp circuitry and further subtracted by the P/−4 method. An unpaired Student's t test was used to evaluate estimated parameters (mean ± SEM or fitted values ± SE of the fit); p values of < 0.05 were considered statistically significant.

Results

Expression and Gating of D2-S6 Mutant Channels. We created lysine mutants in the D2-S6 region of μ1-G783 to μ1-L795 residues. Four of these 13 mutants expressed sufficient Na^+ currents in transfected HEK293t cells for further experiments; these mutants are N784K, L785K, V787K, and L788K (mutants of G783, L786, N789, L790, F791, L792, A793, L794, and L795 expressed poorly, generally <0.5 nA). The current-voltage families were recorded and the peak conductance/voltage curves were constructed (Fig. 2A, right and left, respectively). The activation parameters of these mutant channels were obtained by a curve-fitting program and are included in Table 1. The N784K and V787K mutants display $V_{0.5}$ values similar to those of wild-

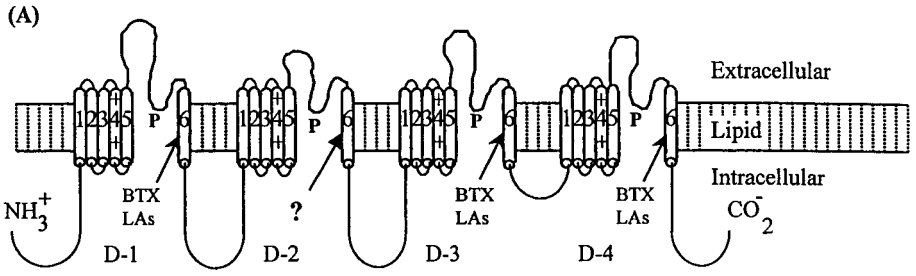

Fig. 1. A, the transmembrane organization of the Na^+ channel α-subunit. The arrows indicate the putative BTX binding site and the putative LA binding site at segment D1-S6, D3-S6, and D4-S6. The role of D2-S6 in BTX and LA action is unknown as labeled by a question mark. *P* designates the pore region within the S5-S6 extracellular linker. B, amino acid sequences of S6 transmembrane segments in domain D1–D4. Residues critical for BTX action are in bold letters. Residues critical for LA binding are underlined. Notice that a total of seven common residues within D1-S6, D3-S6, and D4-S6 are critical for both BTX and LA action.

Downloaded from molpharm.aspetjournals.org by guest on December 1, 2012

type (~−35 mV), whereas L785K and L788K mutants show a significant shift of −5.2 mV and +19.4 mV, respectively ($p < 0.05$).

The steady-state inactivation characteristics (h_∞ curve) of these mutants were determined, as shown in Fig. 2B, and their parameters are listed in Table 1 along with the wild-type for comparison. The $h_{0.5}$ values are similar between wild-type and L788K (~ −84 mV) and are shifted leftward significantly by 6.8 mV for N784K, by 3.7 mV for L785K, and by 8.6 mV for V787K ($p < 0.05$).

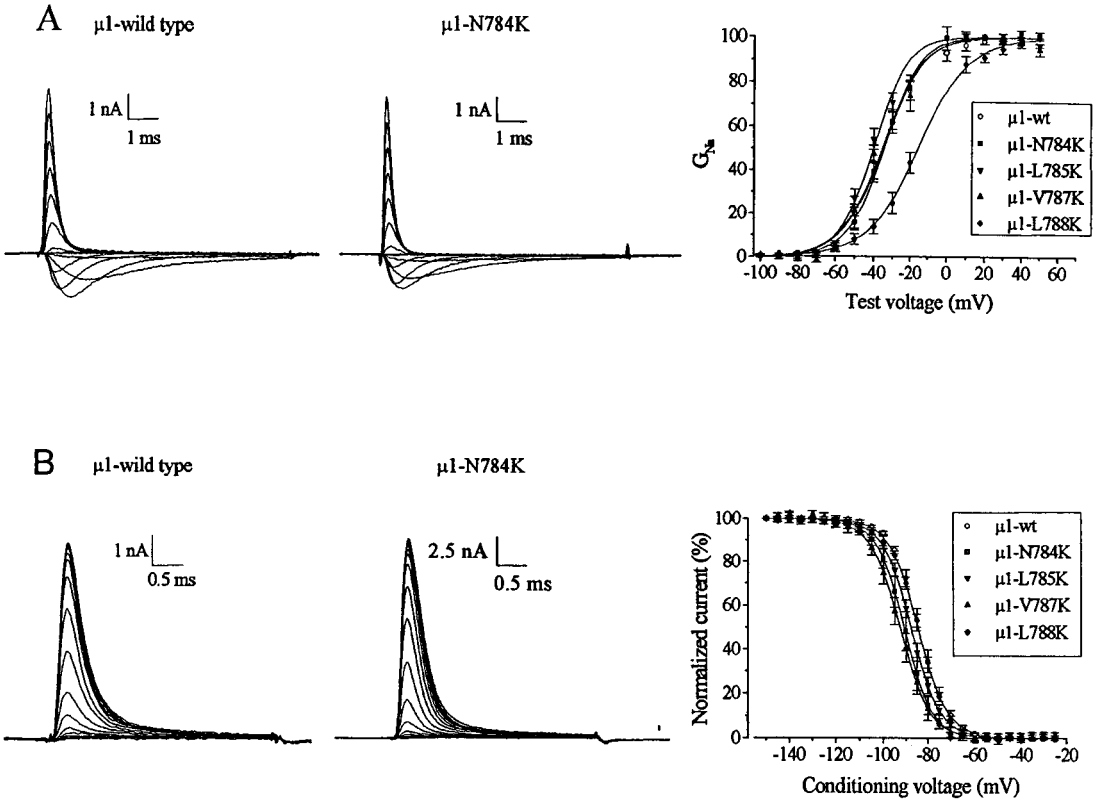

Fig. 2. A, voltage dependence of activation. Mutant and wild-type Na^+ currents were elicited by 4-ms test pulses ranging from −100 mV to +50 mV. Current traces were superimposed (top left). Pulses were delivered in 10-mV increments from a holding potential of −140 mV. Membrane conductance (G_{Na}) was calculated from the equation $G_{Na} = I_{Na}/(E_m - E_{Na})$, where I_{Na} is the peak current elicited by the test pulse, E_m is the amplitude of the test pulse, and E_{Na} is the reversal potential of the Na^+ current. Data were normalized with respect to the maximal G_{Na} (top right) and fitted to a Boltzmann equation: $1 / [1 + \exp (V_{0.5} - V / k_a)]$. The average midpoint voltage ($V_{0.5}$) and slope factor (k_a) for mutant and wild-type channels are shown in Table 1. B, steady-state fast inactivation (h_∞). Na^+ currents were evoked by a 3.6-ms test pulse to +50 mV after 100-ms conditioning pulses (E_C) ranging between −150 mV and −25 mV. The E_C were delivered in 5-mV increments from a holding potential of −140 mV. Pulses were administered at 10-s intervals. Current traces were superimposed (bottom left). Peak currents were measured at +50 mV, normalized with respect to the value at E_C = −150 mV, plotted against the E_C, and fitted to a Boltzmann equation (bottom right). The midpoint voltage for fast inactivation ($h_{0.5}$) and the slope factor (k_h) are shown in Table 1.

TABLE 1

Gating parameters of μl wild-type and mutant Na^+ channels.

The values for the voltage dependence of activation, $V_{0.5}$ and k_a (mean ± S.E.), and fast inactivation, $h_{0.5}$ and k_h (mean ± S.E.) were obtained as described in Fig. 2. Slow gating $s'_{0.5}$ and k'_s (fitted values ± S.E.) in the absence and presence of 100 μM bupivacaine were obtained as described in Fig. 3B. Except for V787K, the $s'_{0.5}$ and k'_s values without drug represent non–steady-state values and therefore are used for renormalization purposes only.

Channel types	μl-WT	N784K	L785K	V787K	L788K
			mV		
Fast gating					
$V_{0.5}$	−34.9 ± 0.7	−34.3 ± 0.5	−40.1 ± 0.7	−35.4 ± 1.2	−15.5 ± 0.5
k_a	11.1 ± 0.7	9.9 ± 0.4	9.2 ± 0.7	11.1 ± 1.2	13.8 ± 0.3
	(n= 8)	(n= 10)	(n= 6)	(n= 9)	(n= 5)
$h_{0.5}$	−84.0 ± 0.1	−90.8 ± 0.1	−87.7 ± 0.2	−92.6 ± 0.2	−84.6 ± 0.2
k_h	6.3 ± 0.1	6.3 ± 0.1	6.5 ± 0.1	6.7 ± 0.1	6.6 ± 0.2
	(n= 6)	(n= 4)	(n= 6)	(n= 5)	(n= 5)
Slow gating (no drug)					
$s'_{0.5}$	−58.7 ± 1.2	−55.0 ± 7.7	−71.3 ± 2.5	−131.5 ± 0.9	N.A.
k'_s	9.2 ± 0.5	21.2 ± 2.0	6.3 ± 2.2	13.9 ± 0.8	N.A.
	(n= 6)	(n= 8)	(n= 6)	(n= 5)	
Slow gating (in 100 μM bupivacaine)					
$s'_{0.5}$	−109.2 ± 0.4	−113.5 ± 0.7	−113.9 ± 0.5	N.A.	−103.8 ± 1.1
k'_s	6.6 ± 0.3	7.6 ± 0.6	6.9 ± 0.4	N.A.	9.0 ± 1.0
	(n= 6)	(n= 8)	(n= 6)		(n= 5)

N.A., not applicable or unable to fit with the equation (L788K). WT, wild-type.

MOL PHARM
MOLECULAR PHARMACOLOGY
aspet
Downloaded from molpharm.aspetjournals.org by guest on December 1, 2012

MOL PHARM

MOLECULAR PHARMACOLOGY

In addition, we used a 10-s conditioning pulse protocol (Fig. 3, inset) that will be used to measure the voltage-dependent binding of bupivacaine described later. One mutant μ1-V787K displays significantly altered gating properties; with a conditioning pulse of −90 mV, less than 10% of Na^+ current remains (Fig. 3, A and B) as if the slow inactivation is enhanced drastically. About 50% of μ1-V787K Na^+ current is slow inactivated at −132 mV (e.g., $s'_{0.5}$; Table 1). This unique mutant also displays a profound use-dependent phenotype in contrast to the wild-type and other lysine mutants in this D2-S6 region. Repetitive pulses at 2 Hz inhibit peak Na^+ currents up to 50% during the first 100 pulses (Fig. 3C, ●) in the μ1-V787K mutant channels, whereas a reduction of less than 10% is found in the wild-type (Fig. 3C, ○). The remaining lysine mutants, like the wild-type, show little or no use-dependent phenotype when compared under identical conditions. These gating alternations in μ1-V787K mutant channels demonstrate that this residue is important for proper gating behavior of the Na^+ channel slow inactivation.

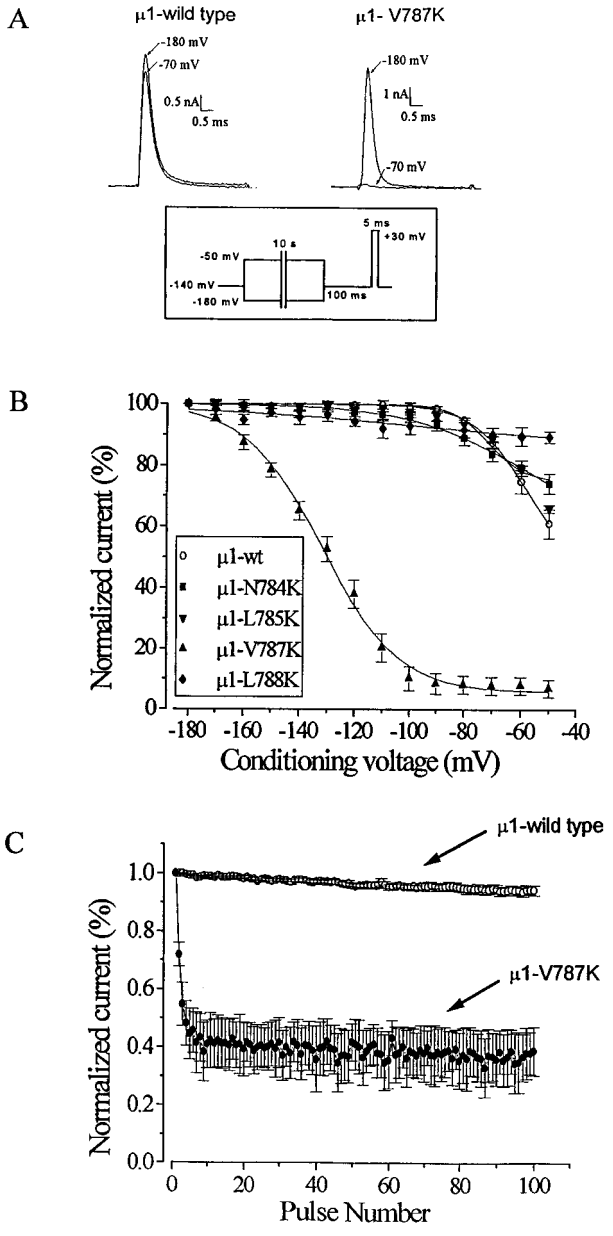

Fig. 3. Prolonged depolarization causes slow inactivation of μ1–787K mutant channels. Cell membranes were kept at a holding potential of −140 mV and received 10-s conditioning pulses ranging in amplitude from −180 mV to −50 mV. A 100-ms interval to −140 mV preceded the 4.4-ms test pulse to +30 mV (see inset). Pulses were delivered at 40-s intervals. Representative current traces were superimposed for comparison (A). Peak currents were normalized to the current evoked by the conditioning pulse of −180 mV, plotted against conditioning voltage (B), and fitted to a Boltzmann equation $[(A1 - A2)/(1 + \exp((E_C - s_{0.5}) / k_s)) + A2]$. The midpoint voltage for inactivation ($s_{0.5}$) and the slope factor (k_s) for each channel are shown in Table 1. Notice that μ1–787K shows a profoundly enhanced slow-inactivation phenotype. C, repetitive pulses also reduce the peak current in the μ1–787K mutant (●, $n = 3$) but not in the wild-type (○, $n = 4$). A 24-ms pulse at +50 mV was applied at 2 Hz for a total of 100 pulses. The peak currents were measured, normalized with respect to the value of the first pulse, and plotted against the pulse number.

BTX-Resistant Phenotype of N784K and L788K. Despite profound gating changes, μ1-V787K mutant channels remained sensitive to BTX. When 5 μM BTX was included in the pipette solution, up to 1000 repetitive pulses produced BTX-modified Na^+ currents that are not inactivated (Fig. 4C as in wild-type, 4A). The peak current amplitude of trace 1000P is about half the size of trace 30P, a result caused by the enhanced use-dependent inhibition of Na^+ current during repetitive pulses. Similar to μ1-V787K, μ1-L785K mutant channels remained sensitive to BTX modification as shown in Fig. 4B. Thus, binding of BTX occurs with mutant channels despite the lysine substitution at these two positions.

In contrast to μ1-V787K and μ1-L785K mutants, adjacent μ1-L788K and μ1-N784K mutants (Fig. 5B and A, left, respectively) became completely resistant to BTX at 5 μM under identical conditions as described in Fig. 4. These results imply that a lysine mutation at either the N784 or the L788 position impairs BTX action drastically. Interestingly, the two residues are roughly oriented at the same face of the proposed α-helical structure. We noticed that repetitive pulses also reduced the peak current of μ1-N784K mutant significantly, albeit with a much slower rate than μ1-V787K (Fig. 5A, left, versus Fig. 4C). The cause of this phenomenon is unclear but could be the alteration of an ultraslow inactivation process.

Previous reports have indicated that the lysine substitution may be important for the activator-resistant phenotype. For example, μ1-F1579K at segment D4-S6 was found both BTX- and grayanotoxin-resistant, whereas μ1-F1579A was not (Wang and Wang, 1999; Kimura et al., 2000). To determine whether the BTX-resistant phenotype of μ1-N784K and L788K is lysine-specific we created μ1-N784C and L788A mutants. We found that both mutants were readily modified by 5 μM BTX after repetitive pulses (Fig. 5, right) as shown for wild-type in Fig. 4A. Therefore, the unique properties of the lysine side chain at position 784 and 788 seem to be critical for the BTX-resistant phenotype.

Bupivacaine Sensitivity of Mutants 784K, 785K, 787K, and 788K. To compare the bupivacaine sensitivity of mutant channels with that of wild-type channels, we used a pulse protocol (detailed in Fig. 3A) to measure the voltage-dependent binding of bupivacaine from −180 mV to −50 mV. A conditioning pulse at various voltages was first applied for 10 s to allow the drug binding to reach the steady state, followed by an interpulse of −140 mV for 100 ms, which allowed drug-free inactivated channels to return to their resting state. The bupivacaine-bound channels recover

Downloaded from molpharm.aspetjournals.org by guest on December 1, 2012

rather slowly with a time constant of 2 to 4 s at −140 mV (Nau et al., 1999). Finally, a test pulse of +30 mV was applied to activate the drug-free resting channels. Figure 6 shows the results for the wild-type channels using this pulse protocol in the absence of 100 μM bupivacaine (Fig. 3B, dashed line). In the presence of 100 μM, at conditioning voltages of −180 to −140 mV, the bupivacaine block was constant about 45% (Fig. 6, ○). This low-affinity bupivacaine block corresponds to the block of the resting state of Na^+ channels. The bupivacaine block increased progressively from voltage −130 to −80 mV until it reached a constant level of ~95% from −70 to −50 mV. This high-affinity bupivacaine block is probably caused by the block of the inactivated state of Na^+ channels. Previous studies have shown that BTX-resistant mutant channels in general have reduced inactivated affinity toward LAs (Nau et al., 1999; Wang and Wang, 1999; Wang et al., 2000). In contrast to this general rule, both 784K and 788K BTX-resistant mutant channels still display comparably high (inactivated) affinity toward bupivacaine. Figure 6 (■ and ♦, respectively) shows the voltage-dependent binding of bupivacaine block in these mutant channels. The $s'_{0.5}$ values are listed in Table 1 along with the wild-type value.

Further measurement of bupivacaine block in 785K mutant channels (Fig. 6, ▲) demonstrates that a lysine substitution of this residue also does not reduce the binding affinity of bupivacaine. Unfortunately, we could not use the same pulse protocol to measure the voltage dependence of inactivated affinity in mutant 787K channels, which seem to have altered slow inactivation (Fig. 3B). Nevertheless, these results together suggest that LAs do not interact directly with μ1–784 and 788 residues within the D2-S6 region. Evidently, both BTX and LAs also do not directly interact with the residue μ1–785.

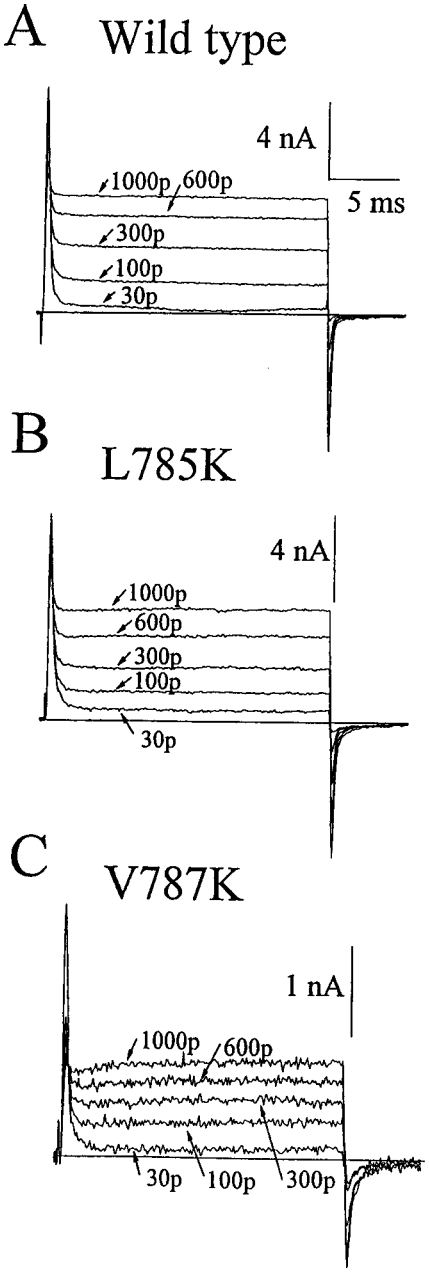

Fig. 4. BTX-sensitive phenotypes of μ1-L785K and μ1-V787K mutants and wild-type. Repetitive pulses at +50 mV for 24-ms at 2 Hz as described in Fig. 3C were applied to cells transfected with wild-type channels (A), μ1-L785K (B), and μ1-V787K (C) mutant channels. The pipette solution contained 5-μM BTX. Outward Na^+ currents were shown at 30, 100, 300, 600, and 1000 pulses, and the current traces were superimposed for comparison. Notice the increase in noninactivating currents and in tail current amplitude after repetitive pulses. Cells were dialyzed by internal solution for 10 to 20 min with infrequent test pulses to determine the peak current amplitude until it reached steady state. Five to six cells of each channel type were used.

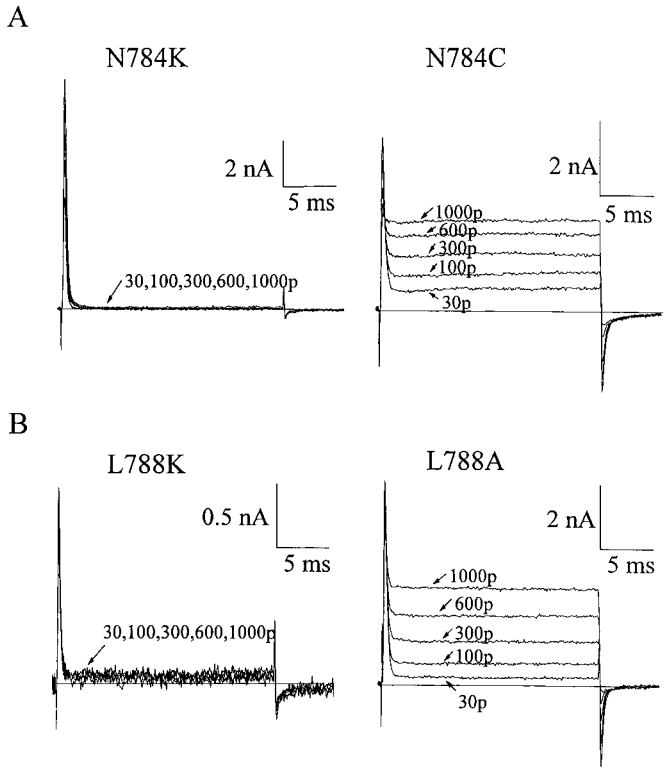

Fig. 5. BTX-resistant phenotype of μ1-N784K and μ1-L788K mutant channels. A pulse protocol identical to that in Fig. 4 was applied to cells transfected with μ1–784K (A, left) and μ1–788K (B, left). Notice the minimal amount of noninactivating currents and tail current after repetitive pulses. In contrast, μ1-N784C and μ1-L788A mutant channels exhibit a BTX-sensitive phenotype (A and B, right). The pipette solution contained 5-μM BTX. Outward Na^+ currents were superimposed for comparison. Five to six cells for each mutant were used. Peak currents in N784K and N784C mutants are significantly reduced during repetitive pulses.

MOL PHARM
MOLECULAR PHARMACOLOGY
aspet
Downloaded from molpharm.aspetjournals.org by guest on December 1, 2012

MOL PHARM
MOLECULAR PHARMACOLOGY
aspet

Dose-Response Curve for K_R and K_I Measurements of Mutant Channels. Knowing the voltage range for the measurement of resting affinity (K_R) and inactivated affinity (K_I) in these lysine mutants, we then proceeded to determine their K_R and K_I values directly at various bupivacaine concentrations at either −70 mV or −160 mV conditioning voltage (Fig. 7). The K_R and K_I values were estimated by curve fitting and are listed in Table 2. Hill coefficient was near unity (p = 1.0 to 1.3) for wild-type and mutant channels, suggesting that there is only one LA binding site within the α-subunit Na^+ channel protein. Our results from dose-response curves further suggest that there are no direct interactions between bupivacaine and residues 784, 785, and 788 within the D2-S6 region. The K_I value for 787K cannot be determined because of its enhanced inactivation gating at −70 mV (Fig. 3, A and B), nor can the K_R value for μ1-V787K be estimated accurately. Although the estimated K_R value for μ1-V787K at −160 mV seems significantly lower than that of the wild-type (Fig. 7B; Table 2), this phenomenon could be caused by inactivated channels at −160 mV conditioning pulse (Fig. 3B).

Discussion

There are two major findings of this report. First, two residues (μ1-N784K and μ1-L788K) within segment D2-S6 of α-subunit Na^+ channels are critical for BTX action but not the two adjacent residues (μ1-L785K and μ1-V787K). Substitution with lysine in either the μ1-L784 or the μ1-V788 position renders the channels completely resistant to 5 μM BTX. Second, although these two specific residues are critical for BTX action, they remain sensitive to bupivacaine block. Similar bupivacaine sensitivities are found in the two mutants μ1-L785K and μ1-V787K. Therefore, no evidence of a strong or a direct contact is found between the D2-S6 residues and LAs.

Implications about BTX Action. Thus far we have identified a cluster of residues at the S6 segments of all four domains that seem to be important for the action of BTX (Fig. 1B). These residues are located near the middle region (position 13 to 21; Fig. 1B) of the S6 transmembrane segment, which contains a total of ~28 amino acids and presumably forms an α-helical structure (Lipkind and Fozzard, 2000). The physiological consequences of BTX poisoning are paralysis, convulsion, and death of the animal. BTX inhibits both fast and slow inactivation of the wild-type Na^+ channel and shifts the voltage dependence of the activation process toward the hyperpolarizing direction, which in turn permits the channel to open persistently even at resting membrane potentials. It is probable that structural perturbations of D2-S6 segment via a lysine point mutation occur either distantly or locally in μ1-N784K and μ1-L788K mutants, which in turn results in the BTX-resistant phenotype. Precisely how the side chain and the α-carbon backbone structural perturbations cause the BTX-resistant phenotype in μ1-

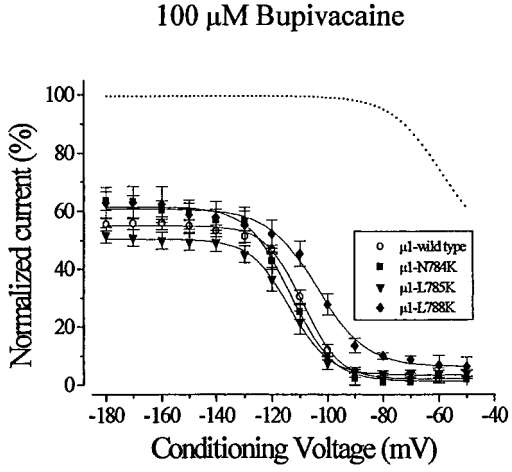

Fig. 6. Steady-state block of wild-type and mutant Na^+ channels by 100 μM bupivacaine. The same pulse protocol as described in Fig. 3A was used in the absence of drug (dashed line for wild-type), and the protocol was repeated after attaining tonic inhibition by 100 μM bupivacaine. Peak currents for each channel were normalized with respect to the control value at the conditioning voltage of −180 mV, plotted against conditioning voltage, and fitted to a Boltzmann equation. The $s'_{0.5}$ and k'_s for the control and drug-bound channels are shown in Table 1 along with $h_{0.5}$ and k_h values.

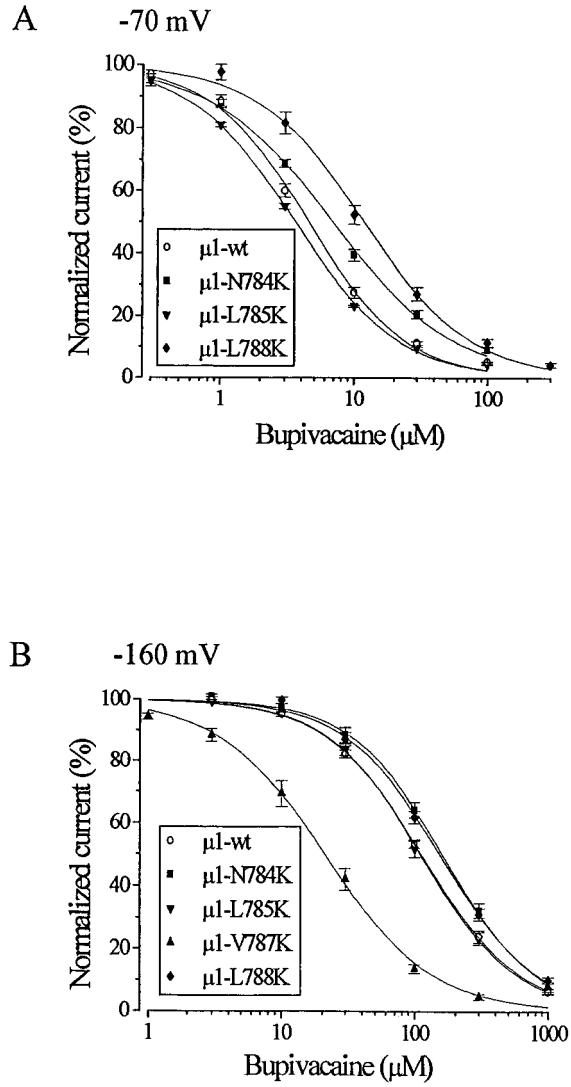

Fig. 7. State-dependent block of μ1 wild-type and mutant Na^+ channels by bupivacaine. The same pulse protocol as described in Fig. 3A was used with conditioning pulses to −70 mV for block of inactivated channels (A) and −160 mV for block of resting channels (B). Pulses were delivered at 30-s intervals. The peak current for each drug concentration was measured, normalized to the peak current in the absence of drug, and plotted against drug concentration. The data were fitted to the Hill equation; the IC_{50} values and the Hill coefficient (p) are listed in Table 2.

Downloaded from molpharm.aspetjournals.org by guest on December 1, 2012

MOL PHARM

MOLECULAR PHARMACOLOGY

N784K and μ1-L788K but not μ1-N784C, L788A, L785K, and V787K mutants remains to be studied.

One hypothesis for the BTX action on Na^+ channel activation is that the lower part of the S6 segment forms part of the activation gate of the Na^+ channel (Wang et al., 2000). Binding of BTX with residues near the activation gate will easily explain the leftward shift of the voltage dependence of activation gating. A possible reason for the inhibition of fast and slow inactivation gating by BTX is the altered or restricted S6 movement in the presence of this toxin (Vedantham and Cannon 2000; Wang et al., 2000). The middle portions of the S6 segments from four different domains could form the lining of the Na^+ permeation pathway (Lipkind and Fozzard, 2000), as suggested by the structure of the KcsA channel (Doyle et al., 1998). The possible rotational and/or lateral movements of S6 segments have been implicated in K^+ channels, which in turn cause the opening and closing of the ion pathway as an inverted teepee architecture (Perozo et al., 1999). If binding of BTX keeps the S6 segments of Na^+ channels in their open configuration, the subsequent movements of S6 segments induced by fast and slow inactivation may therefore be hampered. This restriction of S6 movement implies a coupling between the S6 segment and the inactivation gating processes. It is feasible that structural perturbations of S6 segments by lysine point mutations at specific positions may uncouple this signal transduction pathway and cause the BTX-resistant phenotype.

It is noteworthy that the association rate of BTX with Na^+ channels is state dependent; the open state binds with BTX preferentially, whereas the resting and the inactivated states do so minimally. Therefore, the S6 regions identified so far may likewise hamper the BTX action in a state-dependent manner (Wang et al., 2000). In the closed state, all four S6 segments may trap BTX within the pore region because BTX does not dissociate from its receptor when the BTX-bound channel is closed. In the open state configuration, perhaps only two S6 segments are involved in trapping BTX. The S6 lateral/rotational movement during channel activation may accomplish moving and subsequent trapping of BTX within the domain interface. Otherwise, it will be difficult to explain why ion permeation persists in BTX-modified Na^+ channels if it binds with all four S6 segments simultaneously during depolarization. The BTX receptor, like the LA receptor, must change its conformation during state transitions as reasoned in the modulated receptor hypothesis of Hille (1977). Further experiments to identify the state-dependent contact with BTX are needed before this question can be addressed.

Implications about LA and Insecticide Actions. Although D1-S6, D3-S6, and D4-S6 segments were previously shown to interact with LAs, no such strong interactions have been detected so far between the D2-S6 segment and the LA drugs. Except in D2-S6, all BTX-resistant Na^+ channels display a greatly reduced binding affinity toward LAs (Fig. 1B). In general, a reduction in affinity of ~10- to 20-fold was found for the inactivated state in these channels (Nau et al., 1999; Wang and Wang, 1999; Wang et al., 2000). In contrast, the LA binding affinity of inactivated BTX-resistant Na^+ channels with mutations in D2-S6 segments is quantitatively less affected, ~2.6-fold or less (K_I values of 4.5 μM for wild-type and 11.8 μM for L788K mutant channels). This reduction could be caused by a long-range effect of the positive charge from the lysine residue. Together, these results suggest that the residues within D2-S6 are not as near the bound LA molecule in situ as those within the three other S6 segments. Therefore, the D2-S6 segment represents a unique domain that is critical for BTX but not for LA action. The fact that the LA drugs are smaller molecules than the toxin BTX may be the physical reason why they interact with D1-S6, D3-S6, and D4-S6 but not D2-S6, even in the inactivated state.

Finally, several residues within S6 segments have been mapped to be critical for the pyrethroid-resistant phenotype in insects (e.g., Miyazaki et al., 1996; Williamson et al., 1996; Park et al., 1997; He et al., 1999). Homologous to μ1 channels, these residues are in the following positions: I(V)433 M in D1-S6, L785F(or H) in D2-S6, and F1278I in D3-S6. The I433 position is critical for BTX action (Wang and Wang, 1998) and the L785 position is adjacent to N784, which is critical for BTX action. The F1278I position is two residues away from the S1276 and L1280 positions; both are critical for BTX action. Evidently, S6 segments are also critical for pyrethroid-binding interactions. It is possible that gating changes alone in these insecticide-resistant mutant channels indirectly decrease the pyrethroid binding; hence the insects become resistant to pyrethroid (Vais et al., 1997). Alternatively, pyrethroid insecticide and BTX may bind to distinct but overlapping receptors within the Na^+ channel α-subunit (Vais et al., 2000). Furthermore, these authors also suggest that multiple binding sites are present for pyrethroid insecticide. The physiological consequences of pyrethroid binding to insect Na^+ channels are repetitive firing of neuronal action potentials followed by conduction block, paralysis, and death (Narahashi, 1996). These phenotypes are similar to those of BTX poison; therefore, it is natural perhaps to suggest that these toxins share a common mechanism of action (Hille, 1992) that may occur through interactions with common S6 segments. Significant differences in their actions on Na^+ currents exist between these toxins, but such differences may be explained by their differing structures. If specific S6 segments, individually or combined, are indeed targets of

TABLE 2

Affinities for the resting and inactivated μl wild-type and mutant Na^+ channels.

The 50% inhibitory constant (IC_{50}; fitted values ± S.E.) and p (Hill coefficient) values for the resting ($K_R = IC_{50/R}$) and inactivated ($K_I = IC_{50/I}$) states were determined as described in Fig. 7.

Channel types	μl-WT	N784K	L785K	V787K	L788K
$IC_{50/R}$ (μM)	111.8 ± 1.8	159.7 ± 4.1	109.7 ± 2.1	21.0 ± 0.8	152.8 ± 6.5
p	1.2 ± 0.1	1.3 ± 0.1	1.2 ± 0.1	1.1 ± 0.1	1.2 ± 0.1
	(n= 5)	(n= 4)	(n= 5)	(n= 4)	(n= 6)
$IC_{50/I}$ (μM)	4.5 ± 0.2	6.9 ± 0.3	3.6 ± 0.1	N.A.	11.8 ± 0.7
p	1.2 ± 0.1	1.0 ± 0.1	1.1 ± 0.1	N.A.	1.1 ± 0.1
	(n= 4)	(n= 6)	(n= 4)		(n= 4)

N.A., not applicable; WT, wild-type.

aspet

Downloaded from molpharm.aspetjournals.org by guest on December 1, 2012

various drugs, such as LAs, BTX, antiarrhythmics/anticonvulsants (Ragsdale et al., 1996), antidepressants (Nau et al., 2000), insecticides, and grayanotoxin (Kimura et al., 2000), detailed understanding of this particular region may provide valuable clues for future drug development.

References

Bean BP (1992) Whole-cell recording of calcium channel currents. *Methods Enzymol* **207:**181–193.

Cannon SC and Strittmatter SM (1993) Functional expression of sodium channel mutations identified in families with periodic paralysis. *Neuron* **10:**317–326.

Catterall WA (2000) From ionic currents to molecular mechanisms: the structure and function of voltage-gated sodium channels. *Neuron* **26:**13–25.

Courtney KR (1975) Mechanism of frequency-dependent inhibition of sodium currents in frog myelinated nerve by the lidocaine derivative GEA-968. *J Pharmacaol Exp Ther* **195:**225–236.

Daly JW, Myers CW and Warnick JE (1980) Levels of batrachotoxin and lack of sensitivity to its action in poison-dart frogs (*Phyllobates*). *Science (Wash DC)* **208:**1383–1385.

Doyle DA, Cabral JM, Pfuetzner RA, Kuo A, Gulbis J, Cohen S, Chait BT and MacKinnon R (1998) The structure of the potassium channel: molecular basis of potassium conduction and selectivity. *Science (Wash DC)* **280:**69–77.

Hamill OP, Marty E, Neher ME, Sakmann B and Sigworth FJ (1981) Improved patch-clamp techniques for high-resolution current recording from cells and cell-free membrane patches. *Pflugers Arch* **391:**85–100.

He H, Chen AC, Davey RB, Ivie GW and George JE (1999) Identification of a point mutation in the para-type sodium channel gene from a pyrethroid-resistant cattle tick. *Biochem Biophys Res Commun* **261:**558–561.

Hille B (1977) Local anesthetics: hydrophilic and hydrophobic pathways for the drug receptor reaction. *J Gen Physiol* **69:**497–515.

Hille B (1992) Modifiers of gating. In *Ionic Channels of Excitable Membranes*, pp 445–471, Sinauer Associates, Sunderland, Massachusetts.

Khodorov BI (1978) Chemicals as tools to study nerve fiber sodium channels: effect of batrachotoxin and some local anesthetics. *Prog Biophys Mol Biol* **45:**153–174.

Kimura T, Kinoshita E, Yamaoka K, Yuki T, Yakehiro M and Seyama I (2000) On site of action of grayanotoxin in domain 4 segment 6 of rat skeletal muscle sodium channel. *FEBS Lett* **465:**18–22.

Linford NJ, Cantrell AR, Qu Y, Scheuer T and Catterall WA (1998) Interaction of batrachotoxin with the local anesthetic receptor site in transmembrane segment IVS6 of the voltage-gated sodium channel. *Proc Natl Acad Sci USA* **95:**13947–13952.

Lipkind GM and Fozzard HA (2000) KcsA crystal structure as framework for a molecular model of the Na^+ channel pore. *Biochemistry* **39:**8161–8170.

Miyazaki M, Ohyama K, Dunlap DY and Matsuo H (1996) Cloning and sequencing of the *para*-type sodium channel gene from susceptible and *kdr*-resistant German cockroaches (*Blattella germanica*) and housefly (*Musca domestica*). *Mol Gen Genet* **252:**61–68.

Moczydlowski E, Uehara A and Hall S (1986) Blocking pharmacology of batrachotoxin activated sodium channels. In *Ion Channel Reconstitution* (Miller C ed), pp 405–428, Plenum Press, New York.

Narahashi T (1996) Neuronal ion channels as the target sites of insecticides. *Pharmacol Toxicol* **78:**1–14.

Nau C, Seaver M, Wang S-Y and Wang GK (2000) Block of human heart hH1 sodium channels by amitriptyline. *J Pharmacol Exp Ther* **292:**1015–1023.

Nau C, Wang S-Y, Strichartz GR and Wang GK (1999) Point mutations at N434 in D1–S6 of μ 1 Na^+ channels modulate potency and stereoselectivity of local anesthetic enantiomers. *Mol Pharmacol* **56:**404–413.

Park Y, Taylor MFJ and Feyereisen R (1997) A valine 421 to methionine mutation in I-S6 of the *hscp* voltage-gated sodium channel associated with pyrethroid resistance in *Heliothis virescens* F. *Biochem Biophys Res Commun* **239:**688–691.

Perozo E, Cortes DM and Cuello LG (1999) Structural rearrangements underlying K^+ -channel activation gating. *Science (Wash DC)* **285:**73–78.

Postma SW and Catterall WA (1984) Inhibition of binding of [^{3}H]batrachotoxinin A 20-α-benzoate to sodium channels by local anesthetics. *Mol Pharmacol* **25:**219–227.

Ragsdale DS, McPhee JC, Scheuer T and Catterall WA (1994) Molecular determinants of state-dependent block of Na^+ channels by local anesthetics. *Science (Wash DC)* **265:**1724–1728.

Ragsdale DS, McPhee JC, Scheuer T and Catterall WA (1996) Common molecular determinants of local anesthetic, antiarrhythmic, and anticonvulsant block of voltage-gated Na^+ channels. *Proc Natl Acad Sci USA* **93:**9270–9275.

Strichartz GR (1973) The inhibition of sodium currents in myelinated nerve by quaternary derivatives of lidocaine. *J Gen Physiol* **62:**37–57.

Trimmer JS, Cooperman SS, Tomiko SA, Zhou J, Crean SM, Boyle MB, Kallen RG, Sheng Z, Barchi RL, Sigmworth FJ, Goodman RH, Agnew WS, and Mandel G (1989) Primary structure and functional expression of a mammalian skeletal muscle sodium channel. *Neuron* **3:**33–49.

Vais H, Williamson MS, Goodson SJ, Devonshire AL, Warmke JW, Usherwood PN, and Cohen CJ (2000) Activation of *Drosophila* sodium channels promotes modification by deltamethrin. Reductions in affinity caused by knock-down resistance mutations. *J Gen Physiol* **115:**305–318.

Vais H, Williamson MS, Hick CA, Eldursi N, Devonshire AL and Usherwood PN (1997) Functional analysis of a rat sodium channel carrying a mutation for insect knock-down resistance (kdr) to pyrethroids. *FEBS Lett* **413:**327–332.

Vedantham V and Cannon SC (2000) Rapid and slow voltage-dependent conformational changes in segment IVS6 of voltage-gated Na^+ channels. *Biophys J* **78:**2943–2958.

Wang GK (1988) Cocaine-induced closures of single batrachotoxin-activated Na^+ channels in planar lipid bilayers. *J Gen Physiol* **92:**747–765.

Wang S-Y, Nau C and Wang GK (2000) Residues in Na^+ channel D3–S6 segment modulate batrachotoxin as well as local anesthetic binding affinities. *Biophys J* **79:**1379–1387.

Wang S-Y and Wang GK (1998) Point mutations in segment I-S6 render voltage-gated Na^+ channels resistant to batrachotoxin. *Proc Natl Acad Sci USA* **95:**2653–2658.

Wang S-Y and Wang GK (1999) Batrachotoxin-resistant Na^+ channels derived from point mutations in transmembrane segment D4–S6. *Biophys J* **76:**3141–3149.

Williamson MS, Marinez-Torres D, Hick CA and Devonshire AL (1996) Identification of mutations in the housefly para-type sodium channel gene associated with knockdown resistance (kdr) to pyrethroid insecticides. *Mol Gen Genet* **252:**51–60.

Send reprint requests to: Dr. Ging Kuo Wang, Department of Anesthesia, Harvard Medical School and Brigham & Women's Hospital, 75 Francis St. Boston, MA 02115. E-mail: wang@zeus.bwh.harvard.edu

MOL PHARM
MOLECULAR PHARMACOLOGY
aspet
Downloaded from molpharm.aspetjournals.org by guest on December 1, 2012